Influence of n-type versus p-type AlGaN electron-blocking layer on InGaN/GaN multiple quantum wells light-emitting diodes

Yun Ji, Zi-Hui Zhang, Zabu Kyaw, Swee Tiam Tan, Zhen Gang Ju, Xue Liang Zhang, Wei Liu, Xiao Wei Sun, and Hilmi Volkan Demir

Articles you may be interested in

p-doping-free InGaN/GaN light-emitting diode driven by three-dimensional hole gas
Appl. Phys. Lett. **103**, 263501 (2013); 10.1063/1.4858386

Investigation of surface plasmon coupling with the quantum well for reducing efficiency droop in GaN-based light emitting diodes
J. Appl. Phys. **114**, 113104 (2013); 10.1063/1.4819963

Performance enhancement of blue light-emitting diodes with AlGaN barriers and a special designed electron-blocking layer
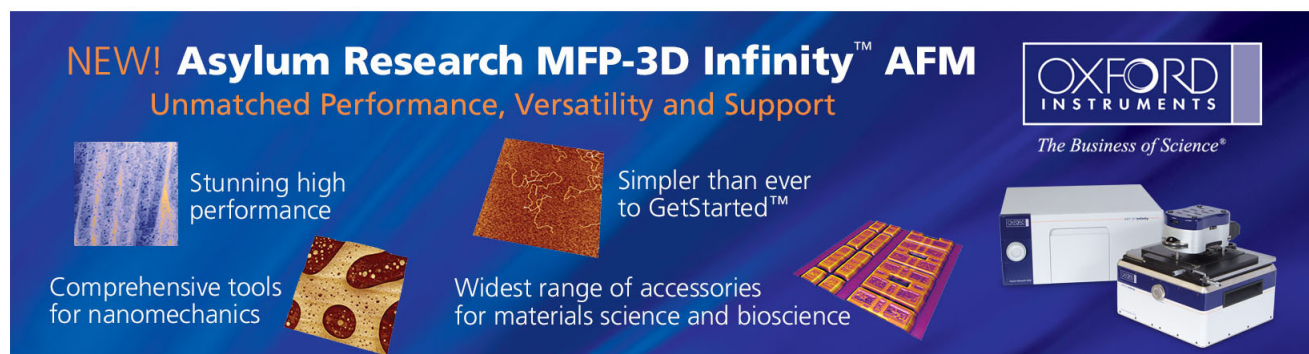J. Appl. Phys. **110**, 093104 (2011); 10.1063/1.3651393

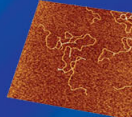Temperature-dependent emission intensity and energy shift in InGaN/GaN multiple-quantum-well light-emitting diodes
Appl. Phys. Lett. **82**, 3614 (2003); 10.1063/1.1578539

Low-temperature operation of AlGaN single-quantum-well light-emitting diodes with deep ultraviolet emission at 285 nm
Appl. Phys. Lett. **81**, 2938 (2002); 10.1063/1.1516631

Influence of *n*-type *versus p*-type AlGaN electron-blocking layer on InGaN/GaN multiple quantum wells light-emitting diodes

Yun Ji,[1] Zi-Hui Zhang,[1] Zabu Kyaw,[1] Swee Tiam Tan,[1] Zhen Gang Ju,[1] Xue Liang Zhang,[1] Wei Liu,[1] Xiao Wei Sun,[1,2,a)] and Hilmi Volkan Demir[1,3,a)]

[1]*LUMINOUS! Centre of Excellence for Semiconductor Lighting and Displays, School of Electrical and Electronic Engineering, School of Physical and Mathematical Sciences, Nanyang Technological University, 50 Nanyang Avenue, Singapore 639798*
[2]*South University of Science and Technology of China, Shenzhen, Guangdong 518055, China*
[3]*Department of Electrical and Electronics, Department of Physics, and UNAM–Institute of Material Science and Nanotechnology, Bilkent University, Ankara TR-06800, Turkey*

The effect of *n*-AlGaN *versus p*-AlGaN electron-blocking layers (EBLs) on the performance of InGaN/GaN light-emitting diodes is studied in this work. Experimental results suggest that the *n*-type EBL leads to higher optical output power and external quantum efficiency, compared to the devices with *p*-AlGaN EBL, which is commonly used today. Numerical simulations on the carrier distribution and energy band diagram reveal that the *n*-AlGaN EBL is more efficient in preventing electron overflow, while not blocking the hole injection into the active region, hence leading to higher radiative recombination rate within the multiple quantum wells active region. © 2013 AIP Publishing LLC. [http://dx.doi.org/10.1063/1.4817381]

InGaN/GaN based light-emitting diodes (LEDs) possess unique advantages including high energy conversion efficiency, long lifetime, compact size, versatile packages, etc. Hence, they are considered the best class of candidate sources to replace the incandescent and fluorescent lighting in the future.[1] Tremendous work has been devoted to improving the performance of InGaN/GaN LEDs addressing various technical challenges.[2] Optical output power and external quantum efficiency (EQE) are the most critical parameters, which need to be further improved in order for the high-power LEDs to penetrate into the consumer market of general lighting.[3–5] One of the limiting factors for the improvement of EQE is electron overflow into the *p*-GaN region and insufficient hole supply into the active region.[6,7] For this purpose, a *p*-type electron-blocking layer (EBL) is commonly adopted to prevent the electron overflow. By inserting a *p*-type doped AlGaN EBL between the multiple quantum wells (MQWs) and the *p*-GaN layer, electrons are confined within the MQWs due to the large potential barrier created by the AlGaN layer, resulting in less electron overflow. To date, different *p*-type EBL structures have been proposed, including the *p*-InGaN/AlGaN EBL,[8] the AlGaN/GaN/AlGaN EBL,[9] and the staircase AlGaN EBL.[10] Although the *p*-type AlGaN EBL is capable of reducing the electron overflow, the large potential barrier height hinders the transport of holes into the MQWs region. This leads to insufficient supply of holes taking part in the radiative recombination with electrons.[11] Therefore, an EBL structure superior to the *p*-type AlGaN EBL is needed, which should be effective in both preventing electron overflow while avoiding the difficulty encountered in hole transport into the MQW region, unlike the conventional *p*-EBL. To this end, an *n*-type doped EBL structure has been theoretically proposed.[12] However, no experimental data or evidence on the improvement of

device performance by the *n*-EBL have been reported in comparison to the commonly employed *p*-EBL to date.

In this work, InGaN/GaN blue LEDs with an *n*-type doped AlGaN EBL was designed and realized. The optical power performance of the InGaN/GaN LEDs with the *n*-doped AlGaN EBL, the *p*-doped AlGaN EBL, and both the *n*-AlGaN and the *p*-AlGaN EBL (*n*-&*p*-AlGaN EBL) structures was comparatively studied. Theoretical simulations were also conducted to reveal the effects of the various types of EBLs on the electron blocking, hole distribution, energy band diagram, and radiative recombination rates in each individual quantum well. The simulation results provide an insightful understanding on the role of the *n*-type AlGaN EBL in achieving better carrier transport and enhancing the optical power performance of InGaN/GaN high power LEDs.

Four InGaN/GaN LED samples (dubbed samples I–IV as sketched in the insets of Fig. 1) were grown on *c*-plane sapphire substrates using metal-organic chemical vapor deposition (MOCVD) system. Trimethylgallium (TMGa), trimethylindium (TMIn), trimethylaluminum (TMAl), and ammonia (NH$_3$) were used as Ga, In, Al, and N precursors, while silane (SiH$_4$) and Bis(cyclopentadienyl)magnesium (Cp$_2$Mg) were used for *n*- and *p*-dopants, respectively. Sample I consists of 5 μm thick unintentionally doped GaN, 3 μm thick *n*-doped GaN (doping concentration $\approx 5 \times 10^{18}$/cm^3), five pairs of InGaN/GaN MQWs, and 200 nm thick *p*-doped GaN (doping concentration $\approx 3 \times 10^{17}$/cm^3). For sample II, a 12 nm thick *p*-doped AlGaN EBL was inserted between the MQWs and the *p*-GaN. On the other hand, for sample III, a 12 nm thick *n*-doped AlGaN EBL was inserted between the *n*-GaN and the InGaN/GaN MQWs. Finally, sample IV consists of both the *n*-doped AlGaN EBL between the *n*-GaN and the InGaN/GaN MQWs and the *p*-doped AlGaN EBL between the *p*-GaN and MQWs. The aluminum content in the EBLs is 15% and the doping concentration is the same as that in the *n*-GaN and the

---

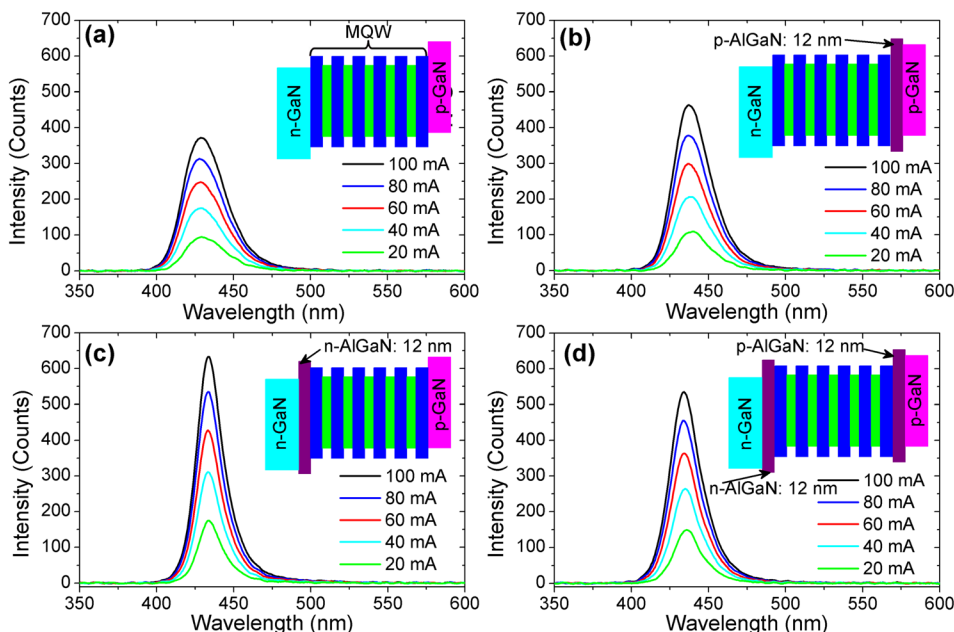a)Electronic addresses: volkan@stanfordalumni.org and exwsun@ntu.edu.sg

FIG. 1. Electroluminescence spectra and device structure diagrams of GaN LED samples: (a) sample I with no AlGaN EBL; (b) sample II with the *p*-AlGaN EBL only; (c) sample III with the *n*-AlGaN EBL only; and (d) sample IV with both the *n*-AlGaN and *p*-AlGaN EBLs.

p-GaN, respectively. After the MOCVD epitaxial growth, the four samples were further fabricated into chips with mesa area of $350 \times 350 \, \mu m^2$. Annealed Ni/Au with a thickness of 5 nm/ 5 nm was applied as transparent current spreading layer, and Ti/Au (30 nm/150 nm) metal bilayer was deposited for both *p*-contact and *n*-contact pads. The LED samples do not include light extraction structures. The electroluminescence (EL) spectra and the optical power of all the fabricated LED chips were measured using an integrating sphere. All characterizations were carried out at room temperature without cooling.

All the LED devices emit blue light with an emission peak at 435 nm, as shown in Figs. 1(a)–1(d). From the EL spectra, it can be found that sample III with the *n*-AlGaN EBL has the highest emission intensity, followed by sample IV with both the *p*-AlGaN and the *n*-AlGaN EBLs, and then sample II with only the *p*-AlGaN EBL. The device with no EBL has the lowest emission peak intensity.

Fig. 2 presents the injection current dependence of the optical output power and the EQE extracted for the four samples. It can be clearly seen that the devices with the electron-blocking layers (sample II, III, and IV) demonstrate superior optical power output and EQE throughout the whole current range measured, compared to the reference device, i.e.,
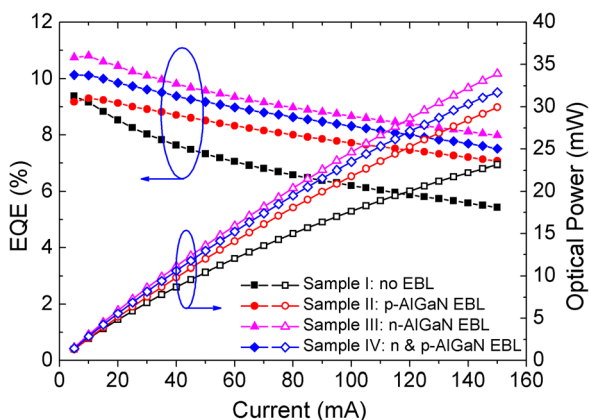

FIG. 2. Measured EQE and optical power of LED samples I–IV.

sample I with no EBL structure. At 150 mA, the optical power of sample I is 23.1 mW, while those of sample II, sample III, and sample IV are 29.9, 33.9, and 31.7 mW, respectively. This result implies that the improvement of the optical output power may be due to the suppression of the electron overflow into the *p*-GaN region by the EBL structures. Among the three samples with the EBLs, sample III exhibits the strongest optical power, in agreement with the EL spectra intensity. The optical power of sample III at 150 mA, and hence the EQE, is about 13.7% and 6.9% higher than those of sample II and sample IV, respectively. The further improvement of the optical output power and the EQE of sample III relative to sample II and sample IV could be due to the different EBLs in the device structures. In order to understand the underlying physics behind the optical performance improvement, theoretical simulations have further been performed to reveal the roles of the different EBLs on the carrier transport, the energy band diagram, and the radiative recombination distribution in the MQWs.

In our numerical simulations, the Poisson equation, the continuity equation, and Schrödinger equation with proper boundary conditions are self-consistently solved using the APSYS software. The self-consistent six-band $k \cdot p$ theory is used to take account of the carrier screening effect in the InGaN quantum wells.[13] The Auger recombination coefficient is taken to be $1 \times 10^{-30} \, cm^6 \, s^{-1}$.[14] The Shockley-Read-Hall (SRH) lifetime for electron and hole is set to be 43 ns.[14] Meanwhile, a 40% of the theoretical polarization induced sheet charge density is assumed due to the crystal relaxation through dislocation generation during the growth. The energy band offset ratio of $\Delta E_C / \Delta E_V = 70/30$ is set in the InGaN/GaN quantum well regions. The other parameters used in the simulation can be found elsewhere.[15,16]

The electron concentration profile within the MQWs active region, under a current density of $120 \, A/cm^2$ ($\approx 150 \, mA$ for $350 \times 350 \, \mu m^2$ device area), is shown in Fig. 3(a). For the device with the *p*-type EBL, the electron concentration is not uniformly distributed and much higher in the first and the last QWs. However, for the device with the *n*-AlGaN EBL, the
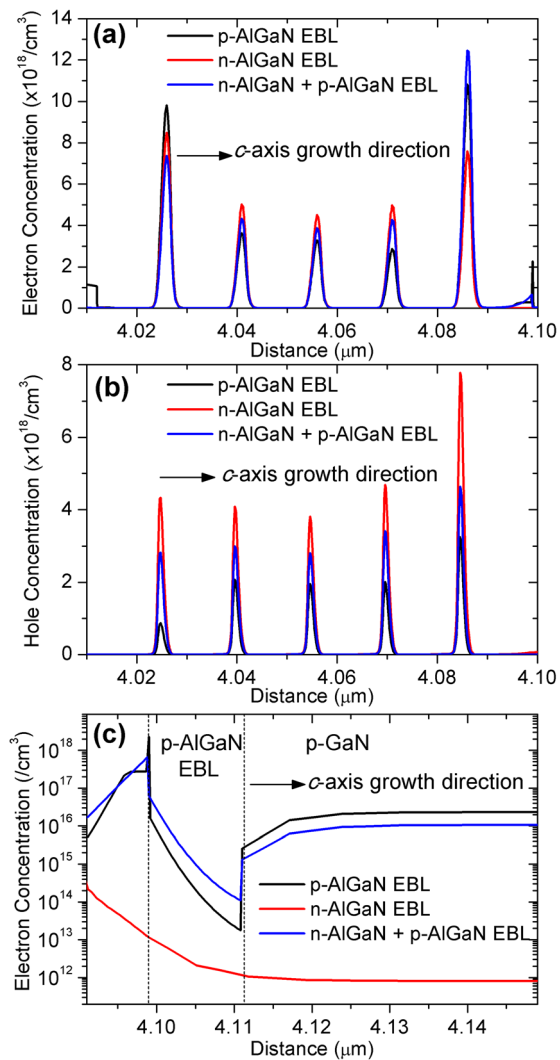
FIG. 3. Simulated electron (a) and hole (b) concentrations within InGaN/GaN MQWs active region, and (c) electron leakage into the *p*-GaN region for LED devices with the *p*-AlGaN EBL (sample II), the *n*-AlGaN EBL (sample III), and the *p*-AGaN + *n*-AlGaN EBLs (sample III) under 120 A/cm² current injection.
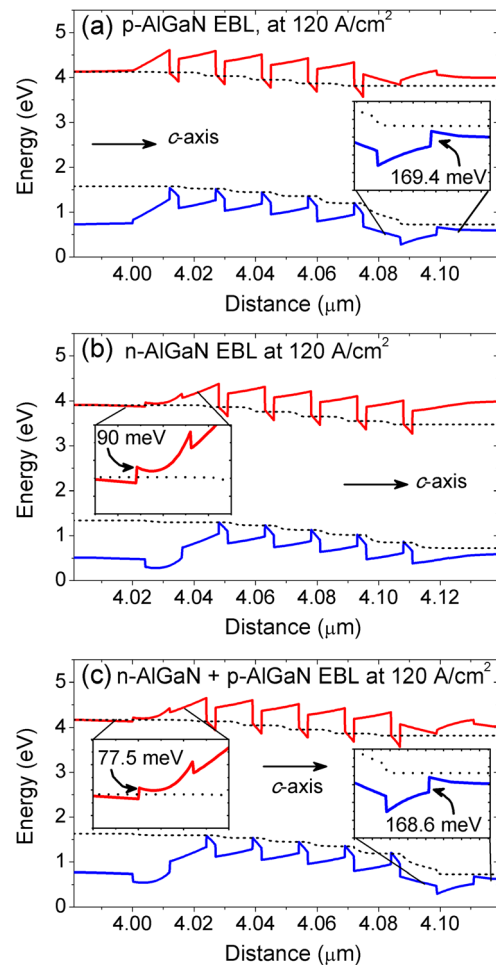

FIG. 4. Simulated energy band diagram for LED devices with (a) the *p*-AlGaN EBL (inset: energy barrier of 169.4 meV height created by the *p*-AlGaN layer in sample II); (b) the *n*-AlGaN EBL (inset: energy barrier of 90 meV height created by the *n*-AlGaN layer in sample III); and (c) the *n*-&*p*-AlGaN EBLs (in sample IV) under 120 A/cm² current injection.

electron distribution is much more uniform, and less electron crowding is observed in the first and the last QWs. When both the *n*-EBL and the *p*-EBL are involved, the device shows better electron concentration uniformity in the first four QWs, but an electron accumulation in the last QW. Fig. 3(b) depicts the hole distributions of the device structures with different EBLs. It can be clearly seen that for the *n*-EBL device, the hole concentration in each individual QW is the highest and the most uniform, compared to the devices with the *p*-EBL and the *p*-&*n*-EBL. Fig. 3(c) illustrates the electron concentrations in the *p*-GaN region for the three devices with the different EBL structures. The device with the *n*-type EBL has the lowest electron concentration in the *p*-GaN region, meaning that the electron overflow into the *p*-GaN region is the lowest here. Therefore, the electron blocking effect of the *n*-AlGaN EBL is found to be more effective than the *p*-EBL and the *p*-&*n*-EBLs.

The simulated energy band diagrams for the LED samples with the different EBL structures, as shown in Figs. 4(a)–4(c), indicate that the carriers are confined within the InGaN/GaN MQWs active region due to the energy barriers

created by the AlGaN layers, which have a larger band gap. The *p*-type EBL, as depicted in Fig. 4(a), creates a potential energy barrier for electrons and hence is able to confine the electrons within the last QW. However, it also generates an energy barrier height of 169.4 meV for holes. In contrast, in the *n*-EBL LED, as shown in Fig. 4(b), the *n*-type AlGaN builds up an energy barrier of 90 meV for electrons before they enter the MQWs active region. Meanwhile, since there is no energy barrier for hole transport into the QWs, n-EBL presents no blocking effect on the hole transport path. When both the *n*-AlGaN and the *p*-AlGaN EBLs are adopted, the energy barriers for both electrons and holes, with the barrier heights of 77.5 and 168.6 meV, are generated, respectively, as illustrated in Fig. 4(c).

Fig. 5 shows the simulated radiative recombination rate of devices with *p*-AlGaN EBL, *n*-AlGaN EBL, and *n*-&*p*-AlGaN EBLs, respectively. The radiative recombination rate within each individual quantum well of the *n*-EBL device is much higher and more uniform than the other two devices. The highest radiative recombination rate occurs in the QW closest to the *p*-GaN layer, owing to the high hole concentration in this quantum well. The characteristic of the radiative recombination rate of the device with the *n*-EBL, in comparison with the *p*-EBL device and the *p*-&*n*-EBL
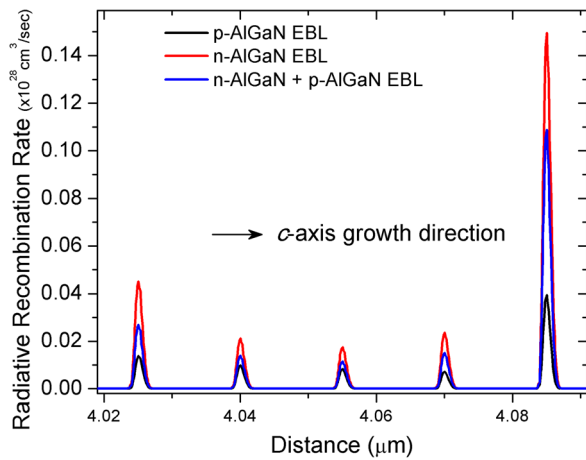
FIG. 5. Simulated radiative recombination rate within the InGaN/GaN MQWs region for LED samples with the *p*-AlGaN EBL (sample II), the *n*-AlGaN EBL (sample III), and the *n*-AlGaN + *p*-AlGaN EBLs (sample IV).

FIG. 6. Measured I–V characteristics of LED samples I–IV.

device, is a consequence of the higher and more uniform electron and hole concentrations within the multiple quantum wells region.

Based on the experimental and the simulation results above, it is understandable that the *n*-type EBL is more effective in reducing the electron overflow and homogenizing both the electron and the hole distributions compared to the *p*-type EBL and the *p*-&*n*-type EBLs. Thus, the *n*-EBL leads to higher radiative recombination rate in the InGaN/GaN MQWs than the *p*-EBL and the *p*-&*n*-EBLs. For sample II with the typical *p*-EBL, the electron concentration in the first QW is higher due to the proximity to the electron injection layer, while the electron concentration in the last QW close to the *p*-AlGaN EBL is also higher as a result of the blocking effect of the high potential barrier of the *p*-AlGaN EBL. Meanwhile, the *p*-AlGaN EBL creates a large potential barrier for holes, making holes transporting into the InGaN/GaN MQWs region more difficult and leading to very severe decay in hole concentration in the region deeper into the active layer. The non-uniform carrier distribution leads to the smaller and non-uniform distribution of the radiative recombination rate in the MQWs for sample II with the *p*-EBL. On the contrary, for sample III with *n*-EBL, the large potential barrier of the *n*-AlGaN EBL mitigates the electron concentration in the first QW, and also there is no large potential barrier blocking the electrons in the last QW near the *p*-GaN region unlike the case of sample II with the *p*-AlGaN EBL. Thus, the electron crowding is insignificant. The electron distribution is more uniform across the whole InGaN/GaN MQWs region. Moreover, the absence of the *p*-EBL allows holes to transport deeper into the active region, resulting in a more uniform hole distribution in each individual QW. The concentrations of electrons and holes in each individual QW are well balanced and matched in sample III. Therefore, the radiative recombination rate in sample III is much stronger and more uniform than that in sample II. The increased radiative recombination rate in the InGaN/GaN MQWs region suppresses the electron overflow as more carriers are consumed there. This explains the superior optical performance of sample III compared to that of sample II. However, after adding the *p*-EBL structure into the device
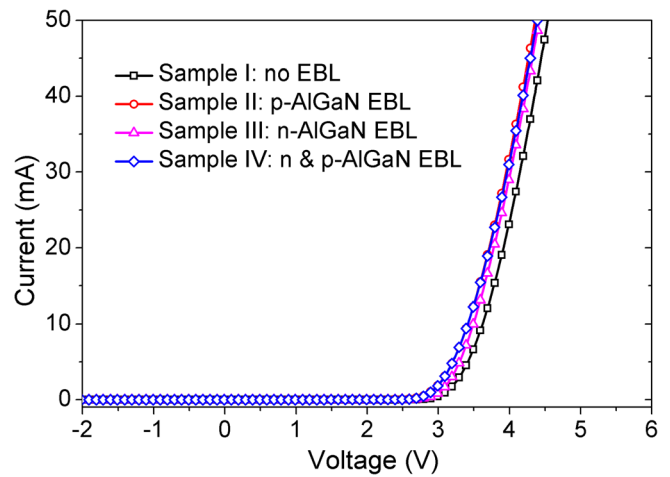
with the *n*-EBL as in the case of sample IV, although the electron concentration in the first QW is further reduced, the electron concentration in the last QW becomes much larger due to the large potential barrier of the *p*-AlGaN. At the same time, the hole transport becomes difficult because of the added *p*-AlGaN EBL, and the hole concentration in the MQWs is smaller than that of sample III. Therefore, the radiative recombination rate of sample IV is reduced compared to that of sample III. That is why when both the *n*-EBL and the *p*-EBL are adopted in sample IV, the device performance is degraded instead of being improved.

The I-V characteristics of samples I–IV were measured and presented in Fig. 6. All the samples with the EBLs (samples II, III, and IV) show a lower forward voltage than the device without any EBL structure. The improved electrical performance is attributed to the enhanced lateral current spreading, due to the large potential barrier created by the AlGaN layer. No obvious difference is observed between the devices with the different EBLs, indicating that with the proper thickness and the doping profile, the EBL will not degrade the device's electrical performance.

In conclusion, the influence of the *n*-type and the *p*-type AlGaN electron blocking layers is comparatively investigated. Both the experimental and the simulation results reveal that the *n*-AlGaN EBL is more efficient in blocking the electron overflow, while not suppressing the hole injection into the active region. The enhanced hole concentration and the uniform carrier distribution within the InGaN/GaN MQWs region result in a higher radiative recombination rate and the improved light conversion efficiency. Hence, the *n*-AlGaN EBL is proved to be more suitable for improving the device performance of high-power InGaN/GaN quantum well light-emitting diodes.

[1]S. Pimputkar, J. S. Speck, S. P. DenBaars, and S. Nakamura, Nat. Photonics **3**(4), 180 (2009).

[2]S. T. Tan, X. W. Sun, H. V. Demir, and S. P. DenBaars, IEEE Photonics J. **4**(2), 613 (2012).

[3]M. H. Crawford, IEEE J. Sel. Top. Quantum Electron. **15**(4), 1028 (2009).

[4]N. Tansu, H. Zhao, G. Liu, X. H. Li, J. Zhang, H. Tong, and Y. K. Ee, IEEE Photonics J. **2**(2), 241 (2010).

[5]Y. Ji, Z.-H. Zhang, S. T. Tan, Z. G. Ju, Z. Kyaw, N. Hasanov, W. Liu, X. W. Sun, and H. V. Demir, Opt. Lett. **38**(2), 202 (2013).

[6]D.-S. Shin, D.-P. Han, J.-Y. Oh, and J.-I. Shim, Appl. Phys. Lett. **100**(15), 153506 (2012).

[7]M.-H. Kim, M. F. Schubert, Q. Dai, J. K. Kim, E. F. Schubert, J. Piprek, and Y. Park, Appl. Phys. Lett. **91**(18), 183507 (2007).

[8]Z. Liu, J. Ma, X. Yi, E. Guo, L. Wang, J. Wang, N. Lu, J. Li, I. Ferguson, and A. Melton, Appl. Phys. Lett. **101**(26), 261106 (2012).

[9]C. S. Xia, Z. M. S. Li, W. Lu, Z. H. Zhang, Y. Sheng, W. Da Hu, and L. W. Cheng, J. Appl. Phys. **111**(9), 094503 (2012).

[10]S.-J. Chang, S.-F. Yu, R.-M. Lin, S. Li, T.-H. Chiang, S.-P. Chang, and C.-H. Chen, IEEE Photonics Technol. Lett. **24**(19), 1737 (2012).

[11]S.-H. Han, D.-Y. Lee, S.-J. Lee, C.-Y. Cho, M.-K. Kwon, S. P. Lee, D. Y. Noh, D.-J. Kim, Y. C. Kim, and S.-J. Park, Appl. Phys. Lett. **94**(23), 231123 (2009).

[12]S.-H. Yen, M.-C. Tsai, M.-L. Tsai, S. Yu-Jiun, T.-C. Hsu, and Y.-K. Kuo, IEEE Photonics Technol. Lett. **21**(14), 975 (2009).

[13]H. Zhao, R. A. Arif, Y.-K. Ee, and N. Tansu, IEEE J. Quantum Electron. **45**(1), 66 (2009).

[14]M. Meneghini, N. Trivellin, G. Meneghesso, E. Zanoni, U. Zehnder, and B. Hahn, J. Appl. Phys. **106**(11), 114508 (2009).

[15]I. Vurgaftman and J. R. Meyer, J. Appl. Phys. **94**(6), 3675 (2003).

[16]Z.-H. Zhang, S. T. Tan, Z. Ju, W. Liu, Y. Ji, Z. Kyaw, Y. Dikme, X. W. Sun, and H. V. Demir, J. Disp. Technol. **9**(4), 226 (2013).